10B.3 SURFACE LONGWAVE RADIATIVE FLUX COMPARISONS BETWEEN SURFACE RADIATIVE BUDGET (SRB) AND THE CALIPSO-CLOUDSAT-CERES-MODIS (CCCM {C3M}) DURING 2007.

A. Viudez-Mora*, Paul W. Stackhouse, Jr and Seiji Kato
NASA Langley Research Center, Hampton, VA

ABSTRACT

This study assesses the surface Longwave Radiative Fluxes (LRFs) estimated by two different projects: the GEWEX (Global Energy and Water Cycle Experiment) SRB (Surface Radiative Budget) Release 3.1 and C3M (CALIPSO-CloudSat-CERES-MODIS). Comparisons between two GEWEX SRB flux algorithms and C3M are made during an overlapping time period for the year 2007. The assessment compares the datasets on an annual averaged zonal and on a 1° x 1° global grid basis. The global mean annual differences between C3M and SRB main longwave algorithm are -1.4±4.4 Wm^{-2} (All-sky) and -2.8±2.4 Wm^{-2} (Clear-sky) for downwelling fluxes, while about -0.8±2.4 Wm^{-2} for upwelling. The overall Cloud Radiative Effect (CRE) at the surface also agrees well with differences 1.4±3.4 Wm^{-2}. The other SRB algorithm agrees similarly well. However, more significant differences up to -10 Wm^{-2} are found in the Polar Regions and up to 10 Wm^{-2} in the Tropical Zones. A matched C3M footprint to $1^{o}x1^{o}$ 3-hourly SRB flux also gives good agreement and will be used in the future to better classify and explain the observed zonal differences.

1. INTRODUCTION

Accurate estimates of the cloud radiative effect are required to better estimate the climate variability on regional and global scales. The radiation budget at the surface is a key interface for energy exchange and therefore for detecting climate change. Surface longwave radiative fluxes are an important component of this terrestrial energy budget, which in the case of global annual averaged Downwelling Longwave Fluxes (DLF), show a disagreement of about 15 Wm^{-2} between different referenced studies (Stephens et al. 2012, Kato et al. 2011, etc).

While direct observations of surface irradiances are limited to ground sites over the land, accurate satellite-based estimations provide an understanding of flux variability at larger spatial scales. To date most satellite based longwave flux algorithms make assumptions regarding the vertical profiles of clouds (Zhang et al., 2004, Gupta et al., 1992, Stackhouse et al., 2011).

New methods, using CALIPSO and CloudSat now specify cloud vertical profiles explicitly (Kato et al, 2011), but are limited in time and space. For an overlapping period of one year (2007), this study assesses the LRFs estimated by two different projects GEWEX SRB (Surface Radiative Budget) and 3CM (CALIPSO-CloudSat-CERES-MODIS).

2. DATASET AND METHODOLOGY

2.1 NASA/GEWEX SRB

The NASA/GEWEX Surface Radiation Budget (SRB) Release-3.0 provides global 3-hourly, daily, monthly/3-hourly, and monthly averages of surface and top-of atmosphere (TOA) longwave and shortwave radiative parameters on a 1°x1° grid. In this study, only the 3-hourly and the monthly averaged surface fluxes are used. Primary inputs to the methods include: International Satellite Cloud Climatology Project (ISCCP) pixel-level (DX) data visible and infrared radiances together with cloud and surface properties derived from those data, temperature and moisture profiles from GEOS-4 reanalysis product obtained from the NASA Global Modeling and Assimilation Office (GMAO, Bloom et al. 2005), and column ozone amounts constituted from Total Ozone Mapping Spectrometer (TOMS), TIROS Operational Vertical Sounder (TOVS) archives, and NOAA's Climate Prediction Center Stratospheric Monitoring-group's Ozone Blended Analysis (SMOBA). Additionally, monthly CO_2 concentrations values are based on monthly trend values from NOAA. For the longwave fluxes two algorithms are used. One of them is an adaptation of Fu et al. (1997), which uses maximum overlap within ISCCP layers of high, middle and low cloud classes and random overlap between those classes. The other method, called LPLA (Langley Parameterization Longwave Algorithm), derives the radiative fluxes described by Gupta et al. (1992).

2.2 CCCM{C3M}

CCCM Edition B1 (CALIPSO-CloudSat-CERES-MODIS) data set is a daily product and contains merged cloud and aerosol vertical profiles

*Corresponding author address:
Antonio Viudez-Mora, NASA Langley Research Center. 21 Langley Boulevard, Mail Stop 420, Hampton, VA 23666.
E-mail: toni.v.mora@nasa.gov

derived from CALIOP (Version 3) and CPR (Revision 4), as well as cloud properties derived from MODIS radiances by the CERES cloud algorithm (Edition3 beta 2). CALIPSO and CloudSat can detect multilayer clouds and aerosol layers overlapping with clouds that are not detected by passive sensors. Merged cloud vertical profiles are collocated with CERES footprints. CERES-derived TOA radiative fluxes (SW, LW, WN) are also included in the product. In addition, cloud properties derived by an enhanced cloud algorithm that uses CALIPSO and CloudSat derived cloud top height combined with the CERES cloud algorithm for improvements are included in the product. Aerosol properties were derived by CALIPSO and MODIS. The radiative fluxes at the surface and in the atmosphere are computed using CALIPSO, CloudSat and MODIS (by enhanced algorithm) derived aerosol and cloud properties as inputs by a radiative transfer model (Flux model for CERES using correlated-K distributions for gaseous absorption - FLCKKR). Temperature and humidity profiles are from the Goddard Earth Observing System (GEOS**-** 4) until October 2007 and GEOS-5 afterwards for Data Assimilation System reanalysis (Rienecker et al., 2008). Because surface radiative fluxes are computed with active sensor derived vertical cloud profiles, surface fluxes improve compared with those computed with passive sensor derived cloud properties alone (Kato et al. 2011).

2.3 Comparison methodology

Based on the different fluxes data sets, three different methodologies are used to assess the surface LRFs. First, we compare the zonal annual averaged fluxes (January to December 2007), from the monthly averaged 1°x1° SRB data products and the C3M footprints that are monthly averaged to 1° zones. It is important to note that due to the nadir collocation of the CALIPSO and CloudSat measurements over each CERES footprint, the C3M daily and monthly averages values represent latitudes from 82° S to 82° N. The second method compares matches C3M longwave fluxes to SRB 3-hourly 1^{o}x1^{o} data products. Each C3M footprint surface longwave flux is matched to the SRB flux from 1°x1° grid box that contains that C3M footprint within ±1.5 hours. Finally, C3M fluxes are compared to SRB fluxes for only those grid boxes that contain a minimum of 5 C3M footprints (Figure 1). Results of the last methods are presented for January and July 2007.

3. RESULTS

The initial comparisons contrast the monthly averaged zonal 1^{o} longwave fluxes from NASA/GEWEX SRB to C3M. The algorithms use similar meteorological input data sets, but the CERES data use the MODIS, CALIPSO and CloudSat derived cloud fields while SRB uses the cloud properties derived from ISCCP for the LPLA and with some overlap assumptions the GEWEX LW.

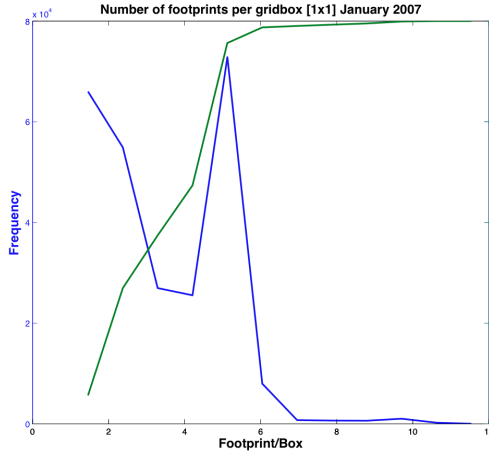

Figure 1: The number C3M footprints within a 1^{o}x1^{o} grid boxes that are matched to SRB fluxes (blue line) and the cumulative distribution of those footprints (green line).

The global annual averaged downwelling longwave fluxes (DLF) at the surface for the two SRB algorithms and for C3M and differences between SRB and C3M for the all-sky and clear-sky cases are shown in Figure 2. This figure shows that the annual zonal profiles for all-sky and clear-sky are similar (top panels). Differences (bottom panels) between each SRB algorithm flux and C3M algorithm are shown the bottom panels. For all-sky conditions (left panels), the largest differences between the datasets occur around the 60° N and S, where the SRB DLF is underestimated compared with C3M. However, in the tropical latitudes, the SRB LPLA DLF overestimates C3M.

The radiative contribution of clouds at the surface can be estimated using the Cloud Radiative Effect (CRE); defined as all-sky DLF minus the clear skies DLF. Figure 3, shows the difference of this CRE for both SRB algorithms (GLW and LPLA) minus the CRE estimated from C3M. Since the SRB algorithms do not account for aerosols effects, the C3M pristine-sky cases (i.e.,, no clouds and no aerosols) are used.

The CRE mean bias difference is 1.4 W m^{-2} for both the SRB GLW and LPLA relative to C3M with zone to zone difference standard deviation of 3.4 and 3.8 W m^{-2} for GLW and LPLA respectively. The positive bias means that both algorithms used in SRB overestimate the radiative effect at the surface compared with C3M. However, the zonal

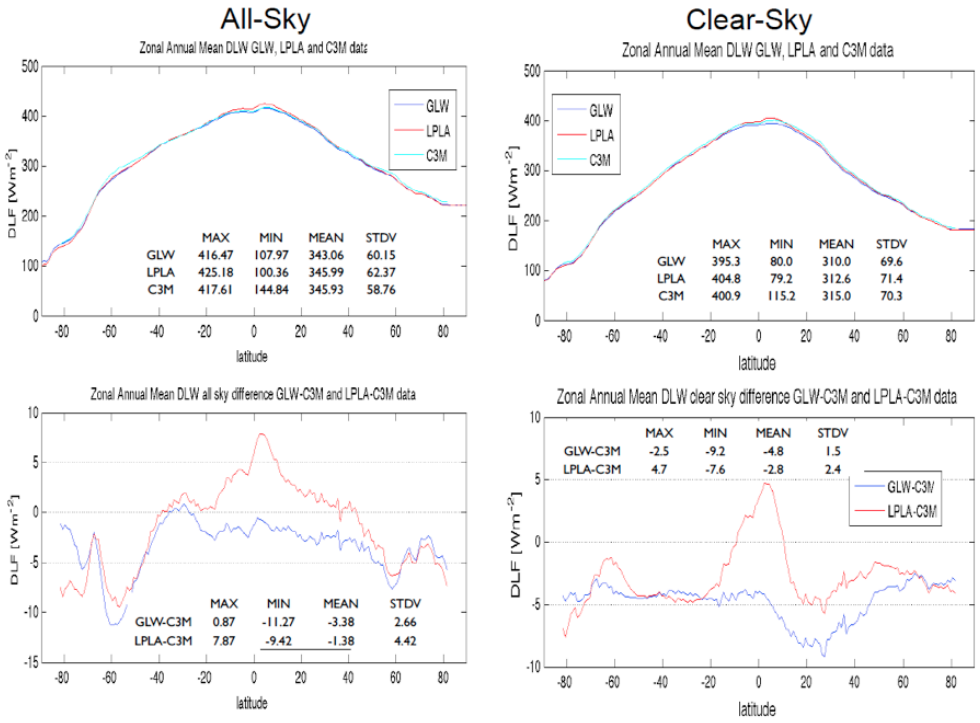

Figure 2: Downwelling longwave fluxes at the surface for all-sky (left) and clear-sky (right) cases. The top panels are the global annual mean zonal profile and bottom are the differences between GEWEX SRB LW (i.e., GLW) and LPLA against C3M. All units are in W m^{-2}.

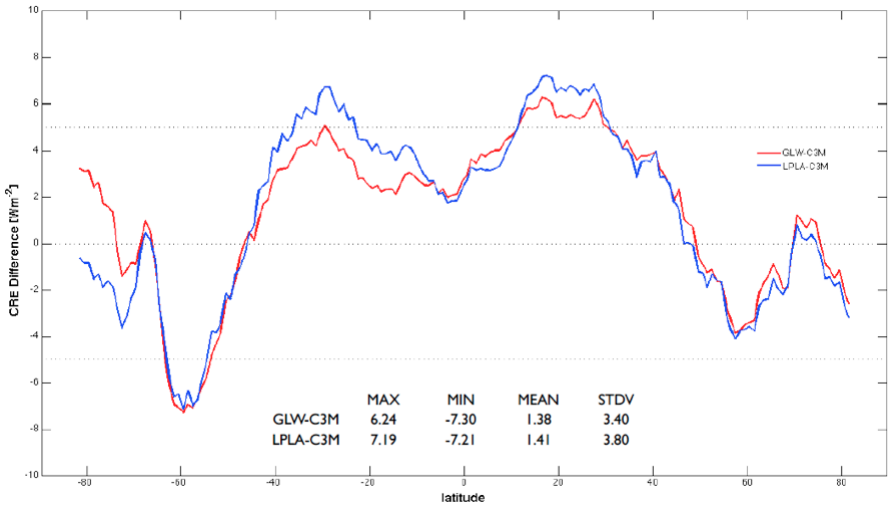

Figure 3: Annual zonal Cloud Radiative Effect average at the surface between SRB (GLW and LPLA) and C3M. Units are in W m^{-2}.

averaged differences show a much larger underestimation near the 60° N/S and an overestimation in the Tropical Zones. So we hypothesize that the GLW and LPLA overestimate the cloud base height and/or the cloud thickness compared with C3M, for latitudes poleward of 40° N (S). For tropical zones, where SRB algorithms overestimate the CRE, the reverse is probably true but will be assessed in future work.

Next, the 3-hourly pair wise methodology was applied for this comparison between datasets. The results are shown for the DLF and ULF fluxes in Figure 4. This figure shows the scatter plots for DLF fluxes in January (top row) and July (bottom row), for all-sky conditions (left column) and clear-sky cases (right column) for 2007. In blue are those GEWEX-SRB grid boxes, which at least have one C3M footprint matched to the SRB longwave flux. Red dots are those GEWEX-SRB grid boxes that

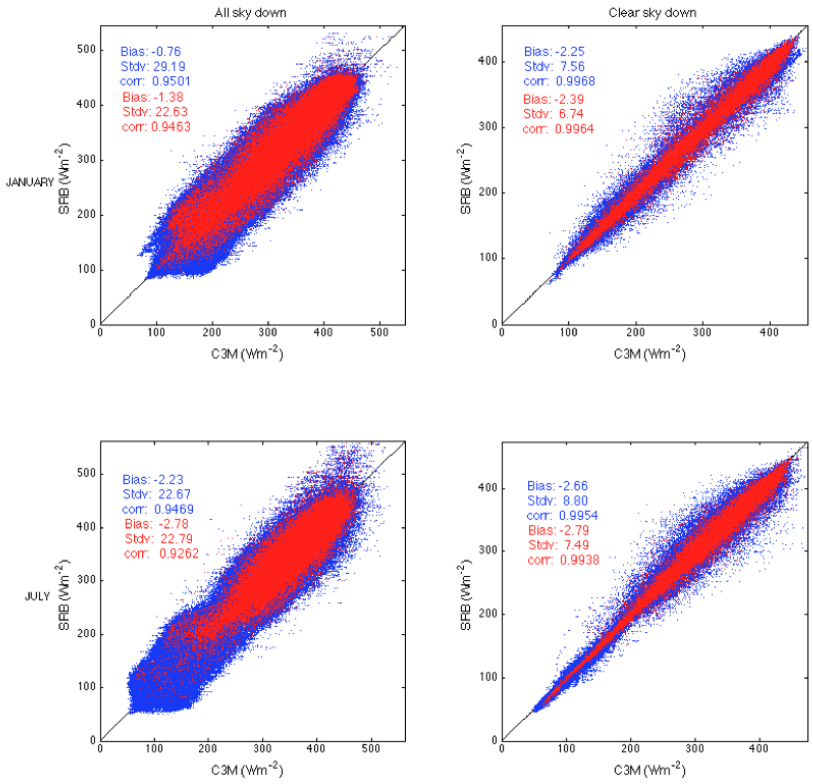

Figure 4: DLF pair wise comparison between GEWEX-SRB and C3M for pair wise unfiltered (blue) and filtered (red) for January (top row) and July (bottom row) 2007 for all skies cases (left column) and clear skies (right column). Units are in Wm^{-2}.

have at least five footprints. Clearly, the most important effect of applying the filtering is the notable noise reduction compared to all matched grid boxes as shown, by the reduction of the standard deviation. The agreement between GEWEX-SRB and C3M is better in clear-sky cases in contrast to all-sky cases where the cloud property assumptions in each algorithm determine the longwave fluxes estimation at the surface.

The matched pair comparison for SRB and C3M are presented for the upwelling longwave fluxes in figure 5. In this figure, as in Figure 4, all C3M/SRB matches are shown in blue and matches restricted to the minimum of 5 C3M footprints are shown in red. The reduction of the standard deviation again shows that requiring the minimum of 5 C3M footprints per grid box improves the comparisons This shows that a larger number of footprints inside the matched grid box are needed to better represent the upwelling surface fluxes..

The green points in Figure 5 show the matched pair ULF comparisons for the special SRB GLW version using only GEOS4 skin temperatures. The formal GLW version uses ISSCP/GEOS-4 surface skin temperature blend that depends on a cloud fraction threshold (i.e., ISCCP skin temperature is used over land when CF<0.5). However, the C3M only uses GEOS4 skin temperatures, so the SRB GLW GEOS4-only skin temperature longwave is more consistent with both the SRB LPLA and the C3M data sets. Indeed the green points show that many of the earlier outliers are removed. This shows the disagreement between the ISCCP and GEOS-4 skin temperatures, particularly in July when much of the northern hemisphere is very hot over dry surfaces. Future work and analysis is needed to better understand the accuracy of these surface skin temperature assumptions.

4. CONCLUSIONS

Overall the agreement between the zonal averaged fluxes and cloud radiative effect is very good. The all-sky bias differences between SRB GLW and LPLA are -3.4 and -1,4 W m^{-2} respectively, Clear-sky biases are of similar sign and given that the CRE are slightly positive (1.4 W m^{-2} for both GLW and LPLA), it's possible that the

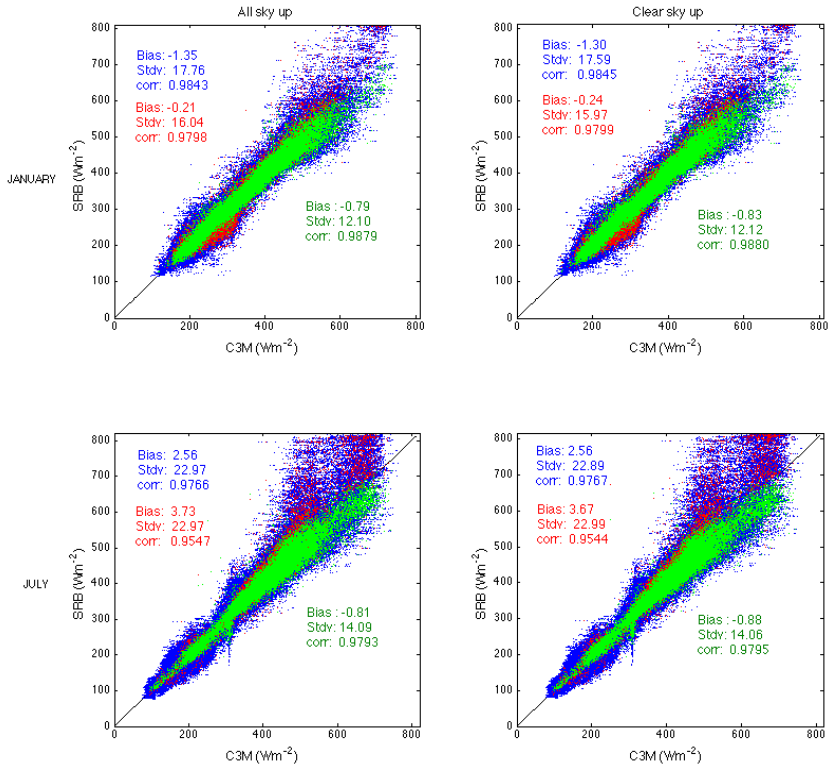

Figure 5: ULF pair wise comparison between GEWEX-SRB and C3M for pair wise unfiltered (blue) and filtered (red) for January (top row) and July (bottom row) 2007 for all skies cases (left column) and clear skies (right column). Units are in Wm^{-2}.

treatment of the meteorological profiles and/or radiative transfer differences between the algorithms is largely responsible for the sign of the all-sky differences. The zonal differences between GEWEX-SRB and C3M are largest (-4 to -8 W m^{-2}) in the Polar Regions most likely due to the different cloud properties in both algorithms. The downwelling fluxes at the surface are strongly dependent on cloud base height. Given that C3M and GEWEX SRB use similar meteorological profiles during the 2007 period, it is plausible that GEWEX SRB under prescribes low clouds from the ISCCP-DX cloud properties. Since the GLW and LPLA differences in these regions are nearly identical, the cloud overlap scheme of the GLW technique is having little effect. By contrast, the active sensing from CALIPSO and CloudSat in C3M better detect the presence of low clouds, particularly when obscured by higher clouds. In the Tropical Regions the reverse could be true that ISCCP low clouds amounts or thicknesses are too high. However, the clear-sky differences indicate that the treatment of the tropical water vapor profiles might also be playing a role, particularly for the SRB LPLA method.

The matched pair differences between C3M and SRG GLW are of similar magnitude as the zonal average fluxes, especially for the all-sky conditions. The differences for upward fluxes are caused by the different the skin temperature assumptions between the methods. Both upward and downward longwave flux difference standard deviations are reduced when the larger scale 1^{o}x1^{o} SRB grid box averages are compared to C3M footprint averages using a minimum threshold. These results show that this technique has potential to better classify and understand differences in terms meteorological and surface conditions.

5. ACKNOWLEDGEMENTS

The authors gratefully acknowledge support by the Surface Radiation Budget Project funded under the NASA Science Mission Directorate Radiation

Sciences program. They also acknowledge the Atmospheric Sciences Data Center of Langley Research Center for access to the NASA/GEWEX SRB and CCCM data set. The main author is granted inside the NPP (NASA Postdoctoral Program) administrated by Oak Ridge Associated Universities.

6. REFERENCES

Bloom, S., A. da Silva, D. Dee, M. Bosilovich, J-D. Chern, S. Pawson, S. Schubert, M. Sienkiewicz, I. Stanjer, W-W. Tan, and M-L. Wu, (2005), Documentation and validation of the Goddard Earth Observing System (GEOS) Data Assimilation System – Version 4. *NASA/TM-2005-104606*, Vol. 26, 187 pp.

Gupta, S. K., W. L. Darnell, and A. C. Wilber, (1992), A parameterization of longwave surface radiation from satellite data: Recent improvements. *J. Appl. Meteorol*., 31, 1361-1367.

Fu, Q., K. Liou, M. Cribb, T. Charlock, and A. Grossman (1997), On multiple scattering in thermal infrared radiative transfer*, J. Atmos. Sci*., 54, 2799–2812.

Kato, S., et al. (2011), Improvements of top-of-atmosphere and surface irradiance computations with CALIPSO-,CloudSat-, and MODIS-derived cloud and aerosol properties, *J. Geophys. Res.,* 116.

Stackhouse, Paul W., Jr., S. K. Gupta, Stephen J. Cox. Taiping Zhang, J. Colleen Mikovitz, and Laura M. Hinkelman, (2011), The NASA/GEWEX Surface Radiation Budget Release 3.0: 24.5-Year Dataset. *GEWEX News*, **21**, No. 1, 10-12, February.

Stephens, Graeme L., Jui-Lin L, Martin Wild, Carol Anne Clayson, Norman Loeb, Seiji Kato, Tristan L'Ecuyer, Paul W. Stackhouse Jr, and Timothy Andrews. (2012). The energy balance of the Earth's climate system (accepted, *J. of Climate*).

Rienecker, M.M., M.J. Suarez, R. Todling, J. Bacmeister, L. Takacs, H.-C. Liu, W. Gu, M. Sienkiewicz, R.D. Koster, R. Gelaro, I. Stajner, and E. Nielsen, 2008: The GEOS-5 Data Assimilation System - Documentation of Versions 5.0.1, 5.1.0, and 5.2.0. *Technical Report Series on Global Modeling and Data Assimilation 104606*, v27.

Zhang, Y., W. B. Rossow, A. A. Lacis, V. Oinas, and M. I. Mishchenko, (2004), Calculation of radiative fluxes from the surface to top of atmosphere based on ISCCP and other global data sets: Refinements of the radiative transfer model and the input data*, J. Geophys. Res.*, 109.